ELECTROSTATIC FORCE IN BLOWING SNOW

D. S. SCHMIDT[1], R. A. SCHMIDT[2] and J. D. DENT[1]
[1]*Department of Civil Engineering, Montana State University, Bozeman, Montana 59717 U.S.A.;*
[2]*USDA Forest Service, Rocky Mountain Research Station, 222 South 22nd Street, Laramie, Wyoming 82070 U.S.A.*

(Received in final form 29 March 1999)

Abstract. Separation of electrostatic charge during the transport of particles by wind adds a force to the gravitational and fluid forces that determine trajectories of particles moving by saltation. Evaluating this electrostatic force requires the electric field strength very near the saltation surface, and charge-to-mass ratios for the moving particles. Field mill readings 4 cm above the surface in a moderate blizzard showed electric field strength as high as +30 kV m^{-1}. Another experiment gave charge-to-mass ratios of individual saltation particles in low-level drifting that ranged between +72 μC kg^{-1} and -208 μC kg^{-1}. From these measurements, we estimated electrostatic forces as large as the gravitational force on some saltating particles. Including forces of this magnitude in the equations of motion significantly alters predicted saltation trajectories from those for uncharged particles. Predictions appear reasonable that for some saltating particles, the electrostatic force prevents new surface impacts. These results should help improve models of energy transfer in the planetary boundary layer during blizzards and sandstorms.

Keywords: Blowing snow, Charge-to-mass, Drifting snow, Electrostatic charge, Electric field, Saltation.

1. Introduction

Static interference on radio antennas prompted early investigations of charge separation in blizzards (e.g., Simpson, 1921; Barre, 1954; Wishart and Radok, 1967). Latham (1964) analyzed available observations on electrification in snowstorms and sandstorms, suggesting that temperature gradients resulting from asymmetric rubbing (Henry, 1953) explained charge separation in both phenomena. Asymmetric rubbing refers to differential heating by friction between small and large surfaces. For snowstorms, temperature gradients in the ice particles produce charge separation because (i) the concentration of H^+ and OH^- ions in ice increases rapidly with increasing temperature, and (ii) H^+ ions are much more mobile within the ice crystal than OH^- ions (Latham and Mason, 1961). As a result, the colder part of an ice particle becomes positively charged, leaving the warmer part charged negatively.

Wind transport of particulates is often divided into three modes, referred to as creep, saltation, and suspension (e.g., Mellor, 1965). Saltation, in which particles bounce through trajectories typically within 10 cm of the surface, is the logical

Boundary-Layer Meteorology **93:** 29–45, 1999.

mode for charge separation by asymmetric rubbing. Saltation is also the logical source for particles that become suspended by turbulence (Radok, 1968), but the mechanisms for this transfer from saltation to suspension remain unclear (e.g., Kind, 1991). Other summaries of developments in the understanding of blowing snow include Radok (1977), Male (1980), Kind (1981), Schmidt (1982), Pomeroy and Gray (1990), and Tabler (1994).

Photographs by Kobayashi (1972, 1987) show that saltating snow particles rebound from elastic impact with stationary surface particles, and follow long, low trajectories in response to forces of fluid drag and gravity. The particles are rounded fragments of the original precipitation crystals, with average diameters most often in the range 0.1 to 0.3 mm (Schmidt, 1981). Using a high-speed camera to photograph saltating glass spheres in a wind tunnel, White and Schulz (1977) found saltation trajectories were higher and longer than predicted using equations involving only fluid drag and gravitational forces. Adding lift created by particle spin to the theoretical equations improved agreement with observed trajectories, with spin rates in the range of 100 to 300 revolutions per second.

An electrostatic force on a charged particle moving in an electric field would also modify saltation trajectories. This force, acting along the electric field vector in the direction determined by the sign of the particle charge, is equal to the product of the electric field and the charge on the particle. Schmidt et al. (1998a) measured the electric field and average charge-to-mass ratio in drifting sand, computing an electrostatic force at 1.7-cm height that was equal in magnitude and opposite in direction to the gravitational force on a 0.15-mm-diameter quartz sphere with positive charge.

Our objective in this paper is to show how the electrostatic force in drifting snow modifies computed saltation trajectories, and to suggest its importance in transferring saltation particles to suspension. As with drifting sand, the computed electrostatic force on particles saltating in moderate blowing snow becomes similar in magnitude to the gravitational force as particles approach the surface. The remainder of this introduction reviews blizzard electrification, and presents equations of motion modified to include the electrostatic force. A second section reviews two experiments in moderate drifting snow, one measuring the electric field, and one determining particle charge-to-mass ratios. The third section combines the experimental results to predict changes in saltation trajectories using the modified equations of motion. Discussion in the fourth section focuses on how modified saltation trajectories might influence the total drift transport.

1.1. ELECTRIFICATION OF BLOWING SNOW

In fair weather, gamma radiation from the ground and from space ionizes air, separating charge and creating an electric field at the Earth's surface. The field is extremely variable, averaging -120 V m^{-1} at 1-m height, where the negative field vector points toward the Earth's centre, indicating positive charge in the atmo-

sphere (Iribarne and Cho, 1980). If the electric field is only a function of height, the relationship between electric field, E, and charge density, λ, is given by Poisson's equation

$$\frac{\mathrm{d}E}{\mathrm{d}y} = \frac{\lambda}{\varepsilon_0}, \tag{1}$$

where y is height above the surface and ε_0 is the permittivity of free space. Integrating expression (1) gives the atmospheric electric field at any height y,

$$E_y = \frac{1}{\varepsilon_0} \int_0^y \lambda \, \mathrm{d}y, \tag{2}$$

as a function of only charge density. (The unit of electric field strength, one Volt per metre (V m^{-1}), is equal to one Newton per Coulomb (N C^{-1}), where Coulomb is the unit of charge.) Rather than the uniform field near an infinite plane of uniform charge, predicted by basic physics when no other charges exist, atmospheric ionization creates a vertical gradient of charge density and electric field strength.

During blizzards, the atmospheric electric field reverses direction and its magnitude increases in the region occupied by blowing particles, indicating excess negative charge density above the surface (Schonland, 1953). Electric field strength diminishes with increasing height in the transport region (Schmidt and Dent, 1994), as expected if excess charge density is associated with the distribution of moving particles.

To estimate the electric field near a saltation surface, Schmidt and Dent (1993) assumed that the surface was a plane of packed spheres with charge equal in magnitude but opposite in sign to the charge on moving particles. Considering the charge of each bed sphere as a point charge at the centre of the sphere, the vertical profile of electric field was estimated by integrating over successively larger circles of spheres, for each height. Figure 1 shows predictions of electric field at the surface as a function of bed sphere diameter for several charge-to-mass ratios. Predicted vertical gradients of electric field increase as surface particles become larger and charge less uniform. Estimated magnitudes of the electric field at the surface compared reasonably well with power-law extrapolations of electric fields reported by Latham and Montagne (1970), when charge on surface particles was taken as the average measured on drifting particles, but with opposite sign. However, while the ice-sphere model is nearer reality than a smooth plane of ice with uniform charge, it is still an extreme idealization of irregular, wind-blown snow surfaces.

Average charge on blowing snow particles, estimated from samples in drift traps designed as Faraday cages, range widely in magnitude, with positive and (more often) negative sign (e.g., Wishart, 1970; Latham and Montagne, 1970). A typical average charge-to-mass ratio by this method is -10 μC kg^{-1}. Schmidt and Schmidt (1992) measured strong positive correlations of average particle charge

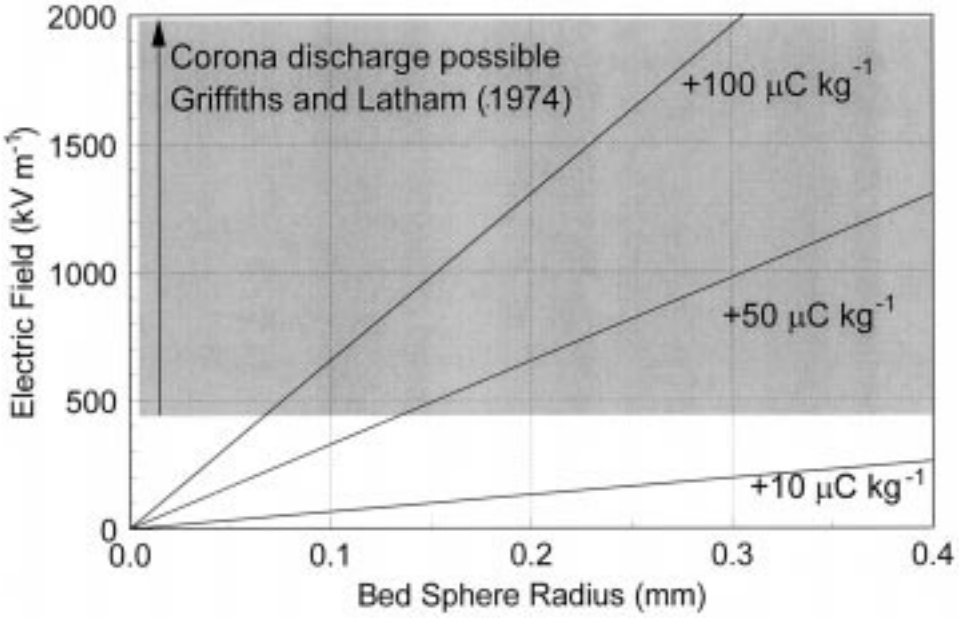

Figure 1. Electric field at the snow surface, predicted by integrating the charge from a plane of ice spheres, with charge-to-mass ratios represented by point charge at each sphere centre (Schmidt and Dent, 1993). Only 61 spheres were included, because contribution to the field decreases rapidly with distance from the centre sphere.

with wind speed and particle flux. However, occasional reversal in sign of measured charge during wind gusts suggested the mixing of eroded surface particles with particles already in transport. Schmidt et al. (1998b) found simultaneous transport of particles with charge of opposite sign, and individual charge-to-mass ratios several times those reported for Faraday cage samples.

Much of what is known about mechanisms of charge separation in ice resulted from efforts to understand electrification in thunderstorms. As noted above, Latham and Mason (1961) demonstrated that temperature gradients in ice produced charge separation. Hobbs (1974, p. 179) reviewed the theory of this process, termed the thermoelectric effect. When a temperature gradient in ice produces an ionic concentration gradient, H^+ ions move more rapidly to colder regions. The process develops a potential difference across uniform pure ice of 2.3 ± 0.3 mV for each °C temperature difference.

Latham and Stow (1967) concluded from laboratory experiments that, in addition to asymmetric rubbing, electrification in blowing snow occurred by crystal fragmentation and by transient contact of particles with different temperatures. The sign and magnitude of charge on particles eroded from a snow surface by an air jet depended strongly on the temperature difference between the jet and the snow. However, for a fixed temperature difference, charging was independent of snow temperature in the range, -10 to -50 °C, and decreased only slightly with

increasing humidity. Particle charging increased by a factor of four with a two-fold increase in jet velocity. A portable field mill that measured the electric field above the eroding snow surface produced erratic results, but showed little field strength when the jet blowing over hard snow was particle-free. With snow particles added to the jet, fluctuations in the field mill readings increased in magnitude, occasionally exceeded 10 kV m^{-1}, and frequently changed sign. Point discharge between highly charged particles was suggested to explain an observed increase in ionization of the surrounding air.

Experiments with corona discharge from ice crystals in the laboratory led Griffiths and Latham (1974) to estimate electric field strength in the range 400 to 500 kV m^{-1} for the onset of corona emissions in thunderclouds. A charged crystal suspended in an electric field by a quartz fibre, discharged initially by a short burst of 10–20 streamers of ionization, released roughly the amount of charge carried by the crystal. The electric field required to produce corona decreased with decreasing pressure from 1000 to 200 hPa, and increased about 4% with a temperature decrease from -4 to -16 °C. Both effects are related to air density and the mean free path of electrons between collisions.

Another mechanism, termed the polarization charging effect, separates charge during the impact of polarized particles in an electric field. Scott and Levin (1970) reviewed developments, beginning with Elster and Geitel (1913), including contributions by Sartor (1954, 1961, 1967), Muller-Hillebrand (1954), and Latham and Mason (1962). The efficiency of the process depends on contact time and the 'relaxation' time required for charge transfer in ice. Impurities in ice reduce the relaxation time, increasing efficiency. When naturally falling snow crystals impacted upon an ice sphere, charge transfer exceeded theoretical predictions in electric fields stronger than 5 kV m^{-1} (Scott and Levin, 1970). The mechanism exhibits positive feedback, as charge separation increases the electric field, which further amplifies charge separation.

Analogous to the increased collection efficiency of falling precipitation crystals with electrostatic charge, it is likely that charged saltating snow particles collect atmospheric trace constituents more efficiently (Pomeroy and Jones, 1996). How this aggregation, and possible solution in the liquid-like layer of the particle surface affects charge, is not yet clear.

Summarizing, charge separation during blizzards produces a mixture of particles with positive and negative charge moving in a strong vertical electric field that decreases rapidly with height above the surface. Most reports show net positive charge on the surface, with net negative charge on moving particles, producing a positive electric field vector, opposite to the fair-weather field. Although several mechanisms are known to separate electrostatic charge in ice, their relative importance in blizzard electrification is still being investigated.

1.2. EQUATIONS FOR SALTATION IN AN ELECTROSTATIC FIELD

White and Schulz (1977) presented equations for saltating motion in which forces acting on the moving particle include fluid drag force, D, lift force, L, and gravitational force, $m_p g$, where m_p is the mass of the particle and g is the gravitational acceleration. Assuming a spherical particle of diameter, d, with charge, q, represented by a point charge at its centre, we have added the electrostatic force, qE, where E is the electric field. In the notation of White and Schulz (1977), the horizontal, vertical, and rotational components of motion for a charged particle saltating in an electric field are

$$m_p \ddot{x} = L\left(\frac{\dot{y}}{V_r}\right) - D\left(\frac{\dot{x}-u}{V_r}\right) + E_x q, \tag{3}$$

$$m_p \ddot{y} = L\left(\frac{\dot{x}-u}{V_r}\right) - D\left(\frac{\dot{y}}{V_r}\right) - m_p g + E_y q, \tag{4}$$

$$I_p \ddot{\theta} = M. \tag{5}$$

Here, u is the velocity of the fluid as a function of height above the surface, I_p is the particle's moment of inertia, $\ddot{\theta}$ is the particle's angular acceleration, and M is the moment acting on the rotating particle. Horizontal and vertical components of the electric field are E_x and E_y. The velocity of the particle relative to the fluid flow, V_r has magnitude

$$V_r = [(\dot{x}-u)^2 + (\dot{y})^2]^{1/2}. \tag{6}$$

Opposing the motion of the particle at this relative velocity, the drag force is expressed in terms of a drag coefficient, C_d, as

$$D = \frac{1}{2} C_d A_p \rho V_r^2, \tag{7}$$

where A_p is the particle cross-section area, and ρ is fluid density.

A lift force results from the pressure difference between the top and bottom of the particle, created by the strong velocity gradient near the surface in the atmospheric boundary layer. This velocity gradient also creates a moment, causing the particle to spin and produce additional lift due to the Magnus effect. Total aerodynamic lift on the particle is

$$L = \frac{1}{8}\pi d^3 \rho V_r \left(\dot{\theta} - \frac{1}{2}\frac{\partial u}{\partial y}\right), \tag{8}$$

where the lift force is coupled to the moment of the particle through the angular velocity $\dot{\theta}$. The moment is

$$M = \pi \mu d^3 \left(\dot{\theta} - \frac{1}{2}\frac{\partial u}{\partial y}\right), \tag{9}$$

with μ denoting fluid viscosity.

For this paper, our solutions of Equations (3)–(5) by numerical methods assumed a semi-logarithmic wind profile, and drag coefficient, $C_d = (24\ Re^{-1})\ (1 - 0.0806\ Re)$, where Re is the Reynolds number based on particle diameter and relative velocity (Carrier, 1953). Although these equations treat total particle charge as a point charge located at the centre of a spherical particle, a distributed charge near the particle surface is more likely.

2. Electric Field and Particle Charge Measurements

This section reviews experiments that measured the two components required to evaluate electrostatic force in drifting snow. An ideal experiment would determine electric field and particle charge simultaneously, but because new techniques were involved, these initial experiments focused on each component separately. Schmidt and Dent (1994) reported preliminary blizzard electric field measurements in the saltation region, and Schmidt et al. (1998b) reported on the charge on individual saltating snow particles.

2.1. ELECTRIC FIELD

Recent miniaturization of field mills for measuring direct-current electric fields allows accurate readings to within a few millimetres of a surface. We used the field meter reported by Johnston and Kirkham (1989), with near-surface corrections from Johnston et al. (1986, Figure 2-22). The sensor is a cylindrical Fiberglass shell 25 mm in diameter and 33 mm long, rotating around the long axis. Two separated semi-cylinders of conductive paint coat the outer surface of the shell. A hybrid microcircuit inside the shell amplifies the oscillating signal generated by the two semi-cylinders spinning in the electric field; this microcircuit converts the signal to a pulse train that is transmitted by optical fibre to a receiver, which demodulates and resolves the signal into horizontal and vertical components of the measured electric field. An air turbine from a dentist's drill rotates the probe at 3000 rpm. The time response of the system is less than 1 s. The probe is at the end of a 1-m long fiberglass tube clamped horizontally to the lower end of the vertical support of an adjustable camera tripod (Figure 2). The sensor height was monitored by a potentiometer on the hand crank of the tripod height adjustment. Tests with and without shielding showed that charged particles impacting the probe had negligible effect on electric field readings, at least for the strong fields of interest in the experiment.

On 6 January 1994, we located a mobile laboratory just south of the Cooper Cove interchange of Interstate Highway 80, 50 km west of Laramie, Wyoming, at 41°3′ N, 106°05′ W, 2360-m elevation. In winter, persistent west winds during frequent drifting, and nearly level terrain with shortgrass vegetation, make the site

Figure 2. Photograph of the senior author checking the height of the electric field mill at the end of experiments on 7 January 1994. Wind sensors (background) were on a short mast downwind and to one side of the electric field measurement.

well suited for blizzard measurements. These surface conditions exist for approximately 1 km upwind of the measuring location, beyond which terrain becomes more rolling for about 3 km, to the foot of the Medicine Bow mountains.

Drifting of a 10-cm new snowfall increased when wind speed became 10 to 17 m s^{-1} at about 0100 h on 7 January. We measured vertical profiles of electric field above the snow surface in the period 0155 to 0739 h by setting the field mill at selected heights in the range 5–37 cm for periods of 10–20 min. Manual measurement of probe height at each change corrected the potentiometer readings for deposition and erosion of the snow surface. When the probe axis was within 5 cm of the surface, erosion directly beneath the probe added uncertainty of about 1 cm to the recorded height. Supporting meteorological measurements included average wind speed, direction, and temperature at 1-m height. The relative humidity sensor was at 2-m height in an enclosure screened with polyester filter fabric, mounted on the side of the mobile laboratory. Measurements were made with respect to water, and probably influenced slightly by the laboratory.

Table I presents the electric field at 22 height settings averaged from 340 readings at 1-min intervals, together with average wind, temperature, and humidity during each height setting. During the 5.5 h of measurement, average wind speed showed no significant trend, wind direction gradually moved about 15 degrees from

TABLE I

Average vertical electric field, E_y, and conditions during sampling periods at fixed field mill heights, on 7 January 1994 in south-eastern Wyoming, U.S.A.

Start (h)	Stop (h)	Height (m)	E_y (kV m^{-1})	Std E_y (kV m^{-1})	Wind speed (m s^{-1})	Std WS (m s^{-1})	Wind Azm (deg)	Temp (°C)	RH (%)
0156	0159	0.10	9.06	3.94	13.03	0.64	285	−12.2	88
0200	0211	0.13	9.59	2.21	12.81	0.88	280	−12.1	88
0212	0225	0.17	5.74	1.37	11.70	0.94	287	−12.0	88
0226	0238	0.05	11.28	3.07	12.44	0.58	287	−11.9	87
0239	0300	0.25	6.51	2.22	13.37	1.11	286	−11.7	87
0301	0317	0.20	6.56	1.93	14.25	0.99	288	−11.6	87
0319	0329	0.05	8.99	5.08	13.95	1.08	282	−11.6	88
0330	0347	0.21	8.63	1.72	14.06	0.91	281	−11.5	88
0349	0403	0.19	8.08	2.19	13.47	1.04	282	−11.4	87
0404	0415	0.16	10.67	2.32	14.60	1.17	281	−11.3	87
0417	0429	0.11	14.92	3.03	13.77	0.99	278	−11.3	87
0433	0445	0.06	11.18	2.93	14.96	0.30	268	−11.1	88
0447	0504	0.11	15.91	2.57	14.67	1.16	272	−11.2	88
0506	0518	0.23	8.85	3.25	13.58	0.99	274	−11.2	87
0520	0534	0.37	3.63	2.13	12.52	0.89	282	−10.9	85
0536	0552	0.09	4.59	2.67	12.34	1.14	282	−10.9	84
0553	0611	0.22	5.68	1.92	12.76	1.27	273	−10.8	85
0612	0632	0.12	7.47	3.19	13.66	1.29	274	−10.6	85
0633	0644	0.08	3.90	3.74	13.53	0.77	269	−10.5	85
0645	0708	0.22	4.71	2.87	12.60	1.24	272	−10.6	85
0709	0724	0.14	9.17	3.09	13.26	0.90	267	−10.5	86
0726	0739	0.09	11.60	3.57	13.87	1.05	271	−10.3	85

north of west to west, air temperature increased from −12.5 to −10.5 °C, and relative humidity decreased slightly (88 to 85%). Towards the end of the measurements, we noted decreased drifting with no wind-speed reduction, indicating that most of the new snowfall was relocated. Samples above both erosion and deposition faces of very small, poorly defined dunes indicated a negative field for only three widely separated readings during the entire measurement period. In a strong gust early in the experiment, we noted a +30 kV m^{-1} instantaneous reading of vertical electric field, E_y, with the probe at 4-cm height. Although we also recorded the much smaller horizontal component of electric field, E_x, we did not record probe orientation (right or left across the wind) in this initial experiment.

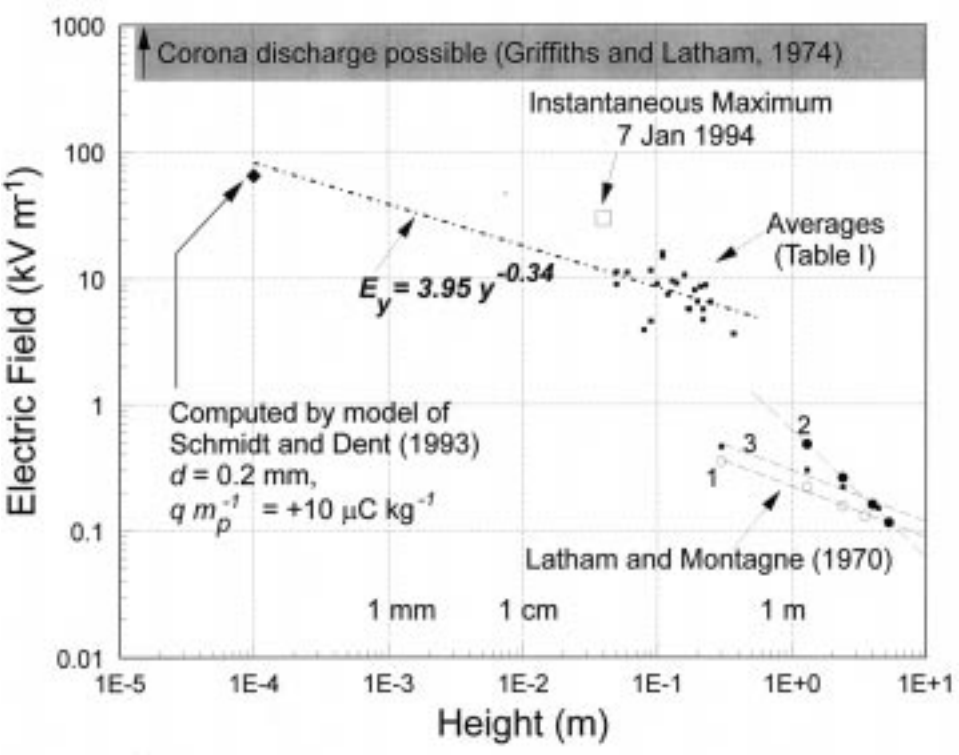

Figure 3. Plot of electric field averages (Table I) compared with measurements of Latham and Montagne (1970) and theoretical predictions from Schmidt and Dent (1993). The power-law fit (dashed line) is extrapolated to the surface in order to estimate saltation trajectories, and may not represent the actual electric field gradient in the near-surface region. The theoretical value at 0.1 mm was not included in the regression fit.

Averages of the vertical electric field, plotted as a function of height in Figure 3, include the strong dependence on wind speed and the change in that dependence with the duration of drifting. Also shown are the measurements of Latham and Montagne (1970) over a snow cornice, and the surface electric field predicted by the distributed charge model of Schmidt and Dent (1993), for 0.2-mm-diameter bed spheres with +10 μC kg^{-1} charge-to-mass ratio. We fitted the power-law profile, $E_y = 3.95\ y^{0.34}$, to data in Table I, and extrapolated it to one particle radius above the surface, only as a first approximation to the electric field gradient for preliminary trajectory evaluations. Note that the theoretical value at 0.1-mm height was not included in the fitted data.

2.2. PARTICLE CHARGE-TO-MASS RATIO

Camp (1976) used a variation of Millikan's oil drop experiment to determine charge-to-mass ratios for falling snow crystals. Based on Camp's methods, Schmidt

Figure 4. Photograph of the experimental setup for initial measurements of charge-to-mass ratios on individual drifting snow particles, showing side view with wind from the right.

et al. (1998b) described an apparatus and experiment to measure the charge on drifting particles. A drift trap extracted snow particles from saltation, and those that did not impact the trap dropped 50 cm into a still-air chamber with a constant horizontal electric field of 148 kV m^{-1}. A detector triggered an imaging system that produced photographs of particle path and location at known time intervals. Particles were deflected horizontally in proportion to their charge, with direction determined by the charge sign. Equations derived by Schmidt et al. (1998b) determined charge-to-mass ratio from particle paths in these images.

Our first measurements with the device in drifting snow provided charge-to-mass ratios of particles in a low-intensity ground blizzard on 8 January 1996 in south-eastern Wyoming. Drifting was channeled along a highway 'right-of-way' through a timber stand at 2770-m elevation. To give vertical clearance for the apparatus, we smoothed a snowplow berm into a ramp that elevated the surface of the 1-m snowpack approximately 1 m (Figure 4). Meteorological data at 1-m height at the drift trap included wind speed, direction, air temperature, and humidity. Although this study site was less than ideal, measured charges on saltating particles probably indicate the range expected for the same saltation rate in less restricted flow.

Saltation began on an old snow surface when wind speed increased to about 8 m s^{-1}. Temperature decreased from +1 to -2 °C soon after drifting began, as

TABLE II

Charge-to-mass ratios of drifting particles determined from deflections in a horizontal electric field during low-level drifting on 8 January 1996 in south-eastern Wyoming, U.S.A. (Schmidt et al. 1998b).

Particle no	Terminal vlocity ($m\ s^{-1}$)	Diameter[a] (mm)	Charge-to-mass ratio ($\mu C\ kg^{-1}$)
1	0.43	0.12	−37
2	0.54	0.13	1
3	0.56	0.14	33
4	0.53	0.13	−12
5	0.51	0.13	32
6	0.34	0.11	27
7	0.57	0.14	72
8	0.59	0.14	−20
9	0.49	0.13	−63
10	0.44	0.12	−208
11	0.63	0.14	−106

[a]Estimated from terminal velocity, assuming a sphere particles 1-4 were on the same image.

complete cloud cover moved in (1300 h). Relative humidity increased to 93% with the cooling, then decreased to 70% as wind speed and drifting moderated. Neither precipitation nor suspended particles were noted during the sampling, from 1400 to 1700 h. A total of 136 images showed 50 particle paths, of which 11 had sufficient clarity and length for estimates of particle charge (Table II). Both left and right deflections in the same photographs confirmed that particles with positive and negative sign were in saltation simultaneously. These initial measurements gave charge-to-mass ratios of individual particles from +72 to -208 $\mu C\ kg^{-1}$, with an estimated uncertainty near 4%. Corresponding equivalent spherical diameters, determined from terminal fall velocities for the two particles at these charge limits, were 0.14 and 0.12 mm, respectively.

3. The Electrostatic Force on Saltating Snow Particles

To estimate the electrostatic force and its effect on saltation trajectories, we combined the measured electric field and charge-to-mass ratios using the equations of motion. As noted above, the field and charge measurements were not simultaneous because the prototype measuring systems each required continuous attention of the two-person field team. However, the measured drifting events were both of light to moderate intensity, and, in our judgement, neither electric field nor particle charge values represent the extremes likely to be measured in more intense blizzards.

We solved the equations of motion, Equations (3)–(5), for a saltating ice sphere, using standard numerical methods with the following assumptions:

(a) particle specific gravity = 0.92, air density = 1.00 kg m^{-3};
(b) initial particle velocity y-component = 0.8 m s^{-1}, x-component = 0;
(c) semi-logarithmic wind speed profile with 0.40 m s^{-1} friction velocity (u_*) and roughness parameter, $z_0 = 0.0015$ m (estimated from snow surface);
(d) particle angular velocity = 0 (no spin, to eliminate Magnus effect);
(e) vertical electric field profile $E_y = 3.95\ y^{-0.34}$ (E_y in kV m^{-1} y in m, Figure 3); $E_x = 0$;
(f) particle charge = +72 μC kg^{-1} and -208 μC kg^{-1}, on particles with 0.14 and 0.12 mm respective diameters (estimated from measured fall velocities).

Solutions are trajectories of the centre of the sphere, so the height at surface contact is equal to the particle radius. The 0.8 m s^{-1} initial vertical velocity (assumption (b)) is based on wind-tunnel measurements of Maeno et al. (1985) and Kikuchi (1981).

Figure 5a compares the calculated trajectories for a 0.12-mm-diameter ice sphere with and without a charge-to-mass ratio of -208 μC kg^{-1}. Figure 5b shows the same comparison for a 0.14-mm ice sphere with and without a positive charge-to-mass ratio of +72 μC kg^{-1}. Using only assumptions (a)–(c), trial-and-error solutions showed that a spin rate of 83 revolutions per second was required for an uncharged particle to match the computed trajectory length of the 0.14-mm ice sphere with positive charge (Figure 5c). For the same particle without spin or charge to match that trajectory length, friction velocity would have to increase from 0.4 to 0.5 m s^{-1}, corresponding to a wind speed increase from 8.8 to 12.1 m s^{-1} at 10-m height. With u_* at 0.4 m s^{-1}, the trajectory length is also matched by decreasing z_0 from 0.0015 to 0.0009 m (not shown in Figure 5).

With a charge-to-mass ratio of -208 μC kg^{-1}, the computed electrostatic force attracting a 0.12-mm-diameter ice sphere to the surface exceeds the gravitational force whenever the particle is within 4 mm above the surface. Again, these computations all assume that the power-law profile (Figure 3) describes vertical electric field strength over the large extrapolation to within one particle radius above the surface (assumption (e) above).

4. Discussion

In the most frequently reported situation, where particles with net negative charge saltate onto a surface with net positive charge, our results predict lower, shorter trajectories as the main effect of blizzard electrification. However, for the smaller fraction of saltating particles with positive charge, computed trajectories are significantly higher and longer. Longer trajectories increase the probability that turbulence moves a particle from saltation into suspension. Particles with posit-

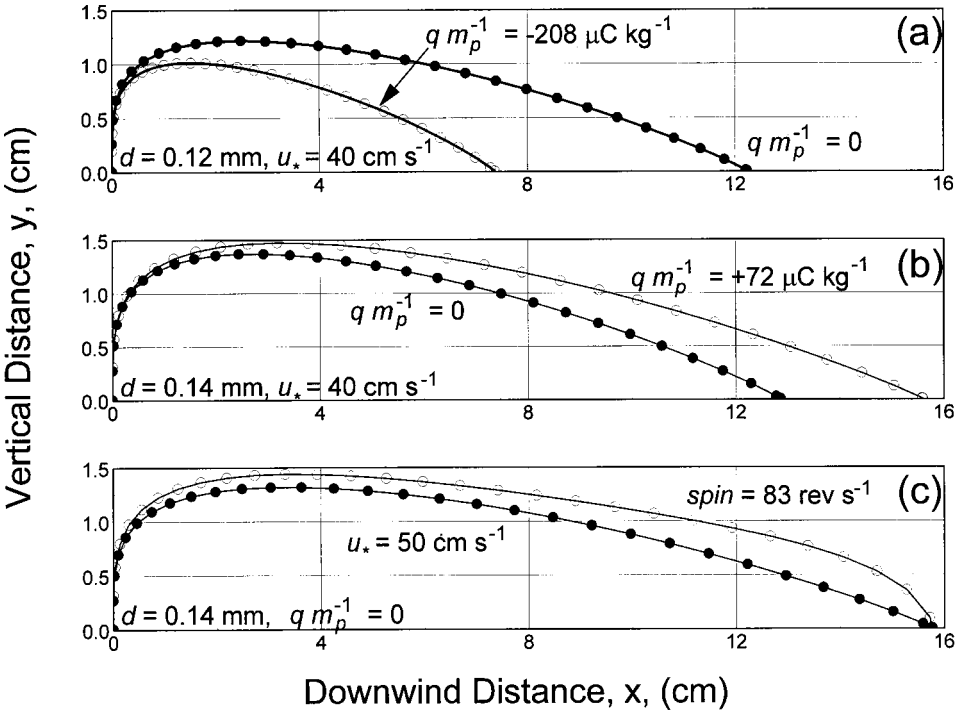

Figure 5. Computed saltation trajectories, (a) for a 0.12-mm-diameter ice sphere with and without a charge-to-mass ratio of -208 μC kg^{-1}, and (b), for a 0.14-mm ice sphere with and without a positive charge-to-mass ratio of +72 μC kg^{-1}. Comparisons in (c) of an uncharged 0.14-mm particle show that spinning at 83 revolutions per second, or increased wind speed, are required to match the trajectory length of the charged particle in (b).

ive charge moving at greater heights tend to moderate the electric field gradient, providing a negative feedback mechanism.

Assuming that additional measurements in more intense drifting will extend our measured range of particle charge (and electric field strength), we were especially interested in trajectory simulations for particles with greater positive charge. Figure 6 shows the computations for a 0.14-mm-diameter ice sphere saltating in the same electric field (assumption (e)), but with positive charge-to-mass ratios greater than the limit of our preliminary measurements (+72 μC kg^{-1}). In general, a particle with sufficient charge-to-mass ratio, $q\ m_p^{-1}$, of the same sign as the net surface charge, moving in a vertical electric field profile described by a power law of the form, $E_y = ay^b$, will seek some equilibrium height, $h = \{g[a(qm_p^{-1})]^{-1}\}^{(1/b)}$, where the vertical electrostatic force balances the gravitational force. If the value of h is high enough such that particle momentum cannot cause surface impact, the particle appears to 'float'. This prediction of floating brings to mind observations of sinuous streams of low-level drifting ('snow snakes') across roadways. The mechanisms that produce 'snow snakes', and the analogous 'sand ropes', may

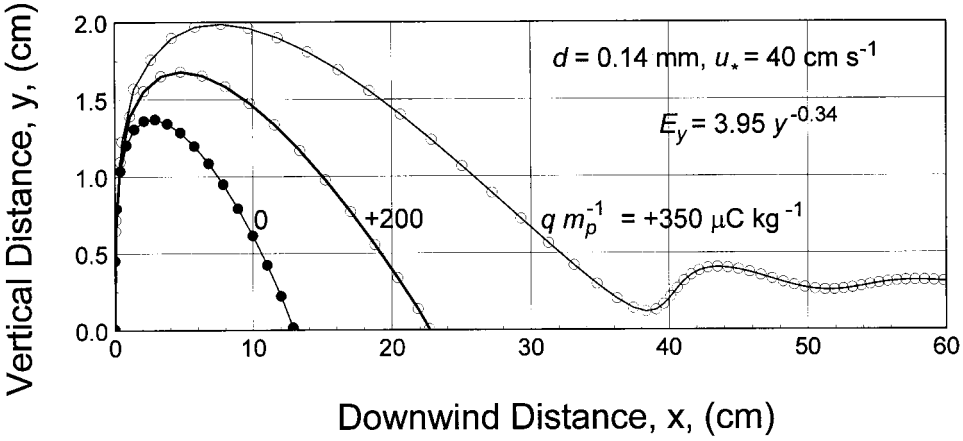

Figure 6. Computed trajectories for a 0.14-mm-diameter ice sphere with positive charge-to-mass ratios greater than the limit of our preliminary measurements (+72 μC kg^{-1}), saltating in the power-law electric field of Figure 3. If stronger electric fields and greater particle charge develop in more intense drifting, it appears possible that some particles may 'float'.

offer an intriguing insight into the decay of atmospheric turbulence. Tests of the electrostatic and alternative hypotheses involving longitudinal vortex pairs should include measurement of the horizontal variation in electric field.

One motivation for our studies of blizzard electrification was curiosity over rapid changes (within 10 min) in the relationship between surface shear stress (or friction velocity, u_*) and the wind-profile roughness parameter, z_0, during drifting (e.g., see Figure 8 in Schmidt, 1986). The measured and computed properties suggest that electrostatic force can alter saltation trajectories enough to change the relationship between the wind-profile parameters, within that time frame. Based on the laboratory experiments of Latham and Stow (1967), it seems possible that an abrupt change in temperature difference between the snow surface and advected air could modify charge separation, changing trajectory heights and the roughness parameter at a given wind speed. We plan to explore such effects more fully in a later study.

5. Conclusions

Separation of electrostatic charge during blizzards produces a mixture of particles with positive or negative charge, moving in electric fields that may become strong enough near the surface to produce corona. Even in moderate drifting snow, the computed electrostatic force near the surface can exceed the gravitational force on saltating particles. Measurements with a miniature field mill showed an electric field 4 cm above an eroding snow surface that reached +30 kV m^{-1}, opposite in direction and greatly enhanced from the fair-weather field. Deflections of drift

particles falling in still air through an electric field provided measurements of particle charge-to-mass ratios. Both left and right deflections in several photographs confirmed the coexistence of drifting particles with charge of opposite sign. Although the relative importance of several mechanisms for charge separation in drifting snow is not yet known, it seems clear that electrostatic forces can strongly affect the relationship between wind speed and snow transport, by modifying saltation trajectories.

References

Barre, M.: 1954, 'Propriétés Électriques du Blizzard', *Résultats Scientifiques* No. S IV, 1, Expéditions Polaires Françaises, Terre Adélie, 1951–1952.

Camp, P. R.: 1976, 'Charge, Morphology, and pH of Natural Snow', *J. Geophys. Res.* **81**(9), 1589–1592.

Carrier, C. F.: 1953, *On Slow Viscous Flow*, Final Report, Office of Naval Research, Contract Nonr-653-00/1, Brown University.

Elster, J. and Geitel, H.: 1913, 'Zur Influenztheorie der Niederschlagselektrizitat', *Phys. Z.* **14**, 1287–1292.

Griffiths, R. F. and Latham, J.: 1974, 'Electrical Corona from Ice Hydrometeors', *Quart. J. Roy. Meteorol. Soc.* **100**, 163–180.

Henry, P. S. H.: 1953, 'The Role of Asymmetric Rubbing in the Generation of Static Electricity', *Brit. J. Appl. Phys.* Suppl. 2, S31–S36.

Hobbs, P. V.: 1974, *Ice Physics*, Clarendon Press, Oxford, 837 pp.

Irbarne, J. V. and Cho, H. R.: 1980, *Atmospheric Physics*, D. Reidel, Norwell, Mass., 212 pp.

Johnston, A. R. and Kirkham, H.: 1989, 'A Miniaturized Space-Potential DC Electric Field Meter', *IEEE Trans. Power Deliv.* **4**(2), 1253–1261.

Johnston, A., Jackson, S., Kirkham, H., and Yeh, C.: 1986, *Power System Applications of Fiber Optic Sensors*, JPL Publ. 86-22, Jet Propulsion Laboratory, Pasadena, CA, U.S.A., 76 pp.

Kikuchi, T.: 1981, 'A Wind Tunnel Study of the Aerodynamic Roughness Associated with Drifting Snow', *Cold Reg. Sci. Tech.* **5**, 107–118.

Kind, R. J.: 1981, 'Snow Drifting', in D. Gray and D. Male (eds.), *Handbook of Snow*, Pergamon Press, Toronto, pp. 338–359.

Kind, R. J.: 1992, 'One-Dimensional Aeolian Suspension above Beds of Loose Particles – A New Concentration-Profile Equation', *Atmos. Environ.* **26A**, 927–931.

Kobayashi, D.: 1972, 'Studies of Snow Transport in Low-Level Drifting Snow', Contributions from the Institute of Low Temperature Science', Hokkaido U., Series A, No. 24, pp. 1–58.

Kobayashi, D.: 1987, 'Snow Accumulation on a Narrow Board', *Cold Reg. Sci. Tech.* **13**, 239–245.

Latham, J.: 1964, 'The Electronification of Snowstorms and Sandstorms', *Quart. J. Roy. Meteorol. Soc.* **90**, 91–95.

Latham, J. and Mason, B. J.: 19761, 'Electric Charge Transfer Association with Temperature Gradients in Ice', *Proc. Roy. Soc. London* **A260**(1303), 523–536.

Latham, J. and Mason, B. J.: 1962, 'Electrical Charging of Hail Pellets in a Polarizing Electric Field', *Proc. Roy. Soc. London* **A266**, 387–401.

Latham, J. and Montagne, J.: 1970, 'The Possible Importance of Electrical Forces in the Development of Cornices', *J. Glaciol.* **9**(57), 375–384.

Latham, J. and Stow, C. D.: 1967, 'A Laboratory Investigation of the Electrification of Snowstorms', *Quart. J. Roy. Meteorol. Soc.* **93**, 55–68.

Maeno, R., Naruse, R., Nishimura, K., Takei, I., Ebinuma, T., Kobayashi, S., Nishimura, H., Kaneda, Y., and Ishida, T.: 1985, 'Wind-Tunnel Experiments on Blowing Snow', *Ann. Glaciol*. **6**, 63–67.

Male, D. H.: 1980, 'The Seasonal Snowcover', in S. Colbeck (ed.), *Dynamics of Snow and Ice Masses*, Academic Press, pp. 305–395.

Mellor, M.: 1965, *Blowing Snow*, CRREL Monograph, Part III, Section A3c, U.S. Army Corps of Engineers, Cold Regions Research and Engineering Laboratory, Hanover, NH, U.S.A., 79 pp.

Muller-Hillebrand, D.: 1954, 'Charge Separation in Thunderstorms by Collision of Ice Crystals with Graupel Falling through a Vertical Electric Field', *Tellus* **6**, 367–381.

Pomeroy, J. W. and Gray, D. M.: 1990, 'Saltation of Snow', *Water Resour. Res.* **26**(7), 1583–1594.

Pomeroy, J. W. and Jones, H. G.: 1996, 'Wind-Blown Snow: Sublimation, Transport and Changes to Polar Snow', in E. Wolff and R. Bales (eds.), *Chemical Exchange between the Atmosphere and Polar Snow*, NATO ASI Series I, Vol 43, Springer-Verlag, Berlin, pp. 453–489.

Radok, U.: 1968, *Deposition and Erosion of Snow by Wind*, U. S. Army Cold Regions Research and Engineering Laboratory, Res. Rep. 230, 23 pp.

Radok, U.: 1977, 'Snow Drift', *J. Glaciol*. **19**(81), 123–129.

Sartor, J. D.: 1954, 'A Laboratory Investigation of Collision Efficiencies, Coalescence and Electrical Charging of Simulated Cloud Droplets', *J. Meteorol.* **11**, 91–103.

Sartor, J. D.: 1961, 'Recalculations of Cloud Electrification Based on a General Charge-Separation Mechanism', *J. Geophys. Res.* **66**, 3070–3071.

Sartor, J. D.: 1967, 'The Role of Particle Interactions in the Distribution of Electricity in Thunderstorms', *J. Atmos. Sci.* **24**, 601–615.

Schmidt, D. S. and Dent, J. D.: 1993, 'A Theoretical Prediction of the Effects of Electrostatic Forces on Saltating Snow Particles', *Ann. Glaciol.* **18**, 234–238.

Schmidt, D. S. and Dent, J. D.: 1994, 'Measurements of The Electric Field Gradient in a Blizzard', *Proc. Int. Snow Sci. Workshop*, Oct. 30–Nov. 3, 1994, Snowbird, UT, U.S.A., pp. 197–202.

Schmidt, D. S. and Schmidt, R. A.: 1992, 'The Sign of Electrostatic Charge on Drifting Snow', *Proc. Int. Snow Sci. Workshop*, Oct 4–8, 1992, Breckenridge, CO, U.S.A., pp. 351–360.

Schmidt, D. S., Schmidt, R. A., and Dent, J. D.: 1998a, 'Electrostatic Force on Saltating Sand', *J. Geophys. Res.* **103**(D8), 8997–9001.

Schmidt, D. S., Dent, J. D., and Schmidt, R. A.: 1998b, 'Charge-to-Mass Ratios of Individual Blowing Snow Particles', *Ann. Glaciol.* **26**, 207–211.

Schmidt, R. A.: 1981, 'Estimates of Threshold Windspeed from Particle Sizes in Blowing Snow', *Cold Reg. Sci. Tech.* **4**, 187–193.

Schmidt, R. A.: 1982, 'Properties of Blowing Snow', *Rev. Geophys. Space Phys.* **20**, 39–44.

Schmidt, R. A.: 1986, 'Transport Rate of Drifting Snow and the Mean Wind Speed Profile', *Boundary-Layer Meteorol.* **34**, 213–241.

Schonland, B. F. J.: 1953, *Atmospheric Electricity*, Methuen, New York, 99 pp.

Scott, W. D. and Levin, Z.: 1970, 'The Effect of Potential Gradient on the Charge Separation during Interactions of Snow Crystals with an Ice Sphere', *J. Atmos. Sci.* **27**, 463–473.

Simpson, G. C.: 1921, *British Antarctic Expedition, 1910–1913*, Vol. 1, Harrison and Sons, London.

Tabler, R. D.: 1994, *Design Guidelines for the Control of Blowing and Drifting Snow*, Strategic Highway Research Program, Report SHRP-H-381, National Research Council, Washington, D.C. 364 pp.

White, B. and Schulz, J.: 1977, 'Magnus Effect in Saltation', *J. Fluid Mech.* **81**(3), 497–512.

Wishart, E. R.: 1970, 'Electrification of Antarctic Drifting Snow', *Proceedings Int. Symposium Antarctic Glaciological Exploration*, Sept. 3–7, 1968, Hanover, NH, U.S.A. IASH Publ. No. 86, pp. 316–324.

Wishart, E. R. and Radok, U.: 1967, 'Electrostatic Charging of Aerial Wires during Antarctic Blizzards', *Polar Meteorology*, Tech. Note No. 87, WMO-No. 211.TP.111, World Meteorol. Organ., Geneva, pp. 492–529.